AUTOMATIC TREE CROWN DELINEATION IN TROPICAL FOREST USING HYPERSPECTRAL DATA

Matheus P.FERREIRA[1], DanielC.ZANOTTA[1],Maciel ZORTEA[2],ThalesS. KÖRTING[1], Leila M.G. FONSECA[1], Yosio E. SHIMABUKURO[1]and Carlos R. SOUZA FILHO[3]

[1]National Institute for Space Research – São José dos Campos – SP – Brazil
(mpf; zanotta; yosio@dsr.inpe.br & thales; leila@dpi.inpe.br)
[2]Norwegian Computer Center – Oslo – Norway (maciel.zortea@nr.no)
[3]Institute of Geosciences, University of Campinas – Campinas – SP – Brazil (beto@ige.unicamp.br)

ABSTRACT

This paper aims to use unique features of hyperspectral data on an automatic process for outlining individual tree crowns (ITCs) in a tropical forest area, with special focus on semi-deciduous species. In order to enhance biophysical and biochemical properties of canopy species, a set of vegetation indices were computed. These indices served as input for a region growing segmentation algorithm that takes into account mutual similarity of pixels and spectral separability between neighbor segments. Segmentation output was evaluated on the basis of a score computed with the proportion of the area of the segments located within manually delineated ITCs. Results show that the segmentation approach is able to automatically delineate up to 70% of the control ITCs.

Index Terms *– Brazilian Atlantic Forest, image segmentation, individual tree crowns, forest management, deciduous tree species*

1. INTRODUCTION

Hyperspectral remotely sensed data provide important information for management and conservation of tropical forests. In this context, research has been developed on tree species discrimination at both leaf- and canopy-levels [1]-[3]. At the canopy-level, due to unique spectral signatures of tree species, the focus has been on pixel-based classification approaches. However, studies performed at the individual tree crown (ITC) level had reported higher classification accuracies [1],[2],[4]. ITCs are often manually delineated using high spatial resolution images [1], since tree crowns, particularly from emergent species, are easily distinguishable. Although this method produces satisfactory results, it is labor intensive and therefore unfeasible over large areas.

Automatic ITC delineation in tropical forests is a challenging task because of the vegetation stands structure. Trees have often non-uniform heights and overlapping crowns, which makes the distinction of clear boundaries between individuals very difficult, even in sub-meter resolution images. Moreover, effects of the bidirectional reflectance distribution function (BRDF) caused by crown architecture, view and illumination angles lead to different proportions of shaded and illuminated pixels within the same ITC. Nevertheless, the information present in hyperspectral images can be exploited to reduce such effects, and enhance spectral features contributing to an improved ITC delineation.

In this work, we propose a method for automatic delineation of tree crowns, in a tropical forest area, using a region growing segmentation algorithm designed specifically for this task. The high dimensionality of hyperspectral data was reduced into a set of vegetation indices (VI) to enhance biophysical and biochemical features of semi-deciduous tree species. The segmentation algorithm took into account, through a spectral separability measure between segments, the contribution of VIs on the automatic ITC delineation process.

2. DATA AND METHODS

2.1 Study area and hyperspectral data

The study area is the reserve of Santa Genebra (22º48'-22°50' S, 47º06'- 47°07' W), located in the municipality of Campinas, in the State of São Paulo, Brazil. The area comprises 251.77 ha and constitutes one of the major remnants of sub-montane semi-deciduous forest (a subtype of Atlantic Forest).

Hyperspectral images were acquired on June 8, 2010 with the ProSpecTIR-VS (AISA Eagle and Hawk) sensor onboard an aircraft flying 1350 m above ground level, resulting in an instantaneous field of view (IFOV) of 1 m. 357 radiance bands were collected in the 400-2500 nm region of the visible and infrared spectra, with a spectral sampling distance of about 5 nm. Ten flight lines cover all the study area.

2.2 Image preprocessing

Prior to the processing steps, the radiance images were georeferenced using a Geographic Lookup Table (GLT) file

and mosaicked, presenting low BRDF effects among scenes. The Fast Line-of-Sight Atmospheric Analysis of Spectral Hypercubes (FLAASH) algorithm [5] was used to convert radiance values into surface reflectance. Three spectrally pure materials (endmembers) comprising "Vegetation", "Soil/Litter" and "Shade" were carefully selected manually, and chosen to model each pixel. The respective fractions were computed using the Linear Spectral Mixing Model (LSMM) [6]. Only pixels containing at least 60% of the component vegetation were further considered for analysis, i.e., pixels dominated by soil/litter and/or shades were masked out. Subsequently, 3 areas of about 400x400 pixels were randomly selected to perform the segmentation tests. These areas were spatially smoothed by a mean filter with a 3x3 moving window to normalize variations of pixel brightness within the ITCs, and to preserve edges simultaneously.

Hyperspectral data provide the possibility to compute several VIs. These indices can enhance biophysical and biochemical features of semi-deciduous canopy tree species. Five VIs were considered in the analysis (Table 1): 1) Normalized Difference Vegetation Index (NDVI) [7]; 2) Pigment Sensitive Normalized Difference (PSDN) [8]; 3) Red-edge Normalized Difference Vegetation Index (RENDVI) [9]; 4) Simple Ratio between Red (600-699 nm) and Green (500-599 nm) broad bands ($SR_{red/green}$)[10]; 5) Structurally Insensitive Pigment Index (SIPI) [11]. To normalize pixel values among VIs, the images were quantized to integers in the 0-255 range.

TABLE I
VEGETATION INDICES SELECTED TO ENHANCE BIOPHYSICAL AND BIOCHEMICAL PROPERTIES OF CANOPY TREE SPECIES

Vegetation Index	Formula
NDVI	$(\rho 864 - \rho 671)/(\rho 864 + \rho 671)$
PSDN	$(\rho 800 - \rho 675)/(\rho 800 + \rho 675)$
RENDVI	$(\rho 752 - \rho 701)/(\rho 752 + \rho 701)$
$SR_{red/green}$	$\overline{\rho}$ RED/ $\overline{\rho}$ GREEN *
SIPI	$(\rho 803 - \rho 467)/(\rho 803 + \rho 681)$

ρ closest ProSpec-TIR bands to the original index formulation
* $\overline{\rho}$ RED and $\overline{\rho}$ GREEN referrers to the mean of all bands in the red range (600-699 nm) and in the green range (500-599 nm), respectively [10].

2.2 Image segmentation

In this work we used a modified version of the region growing segmentation algorithm originally available in the SPRING software [12]. The segmentation starts with an iterative aggregation of pixels presenting mutual similarity in a first order neighborhood. Let i_A and i_B be neighboring pixels with respective neighborhood as depicted in Fig. 1. Both pixels will be merged if, and only if, the most similar neighbor of i_A is $i_{A,2}$ (*i.e.*i_B) and the most similar neighbor of i_B is $i_{B,4}$(*i.e.*i_A). A region is formed if the above mentioned test is true and the spectral Euclidian distance between the two elements is lower than a similarity threshold (T) set by the user.

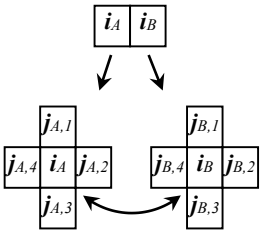

Fig. 1. Analysis of the mutual similarity between two pixels, i_A and i_B.

Another aspect taken into account is the way the threshold value T is handled here. In the same manner as employed in SPRING, the process begins with a T lower than that initially defined by the user and increases at each iteration according to a degree of exigency (*ex*) until T is reached. Considering this reasoning, only the most similar pixels will be merged at first. In this work, a provisory similarity threshold (*p_T*) is updated iteratively by computing *T/ex* ratio. At the last iteration, *ex* is equal to 1.

After merging two pixels, a new region is constructed, an identifier (*id*) is assigned, and the mean value of this region is updated to comply with the new arrangement. In the case of a pixel *i* having another neighbor that already belongs to a region, identified by *id*, its similarity will be calculated over the mean of this region. If the difference between the pixel *i* and this adjacent region is lower than the difference of this pixel among its neighbors, it will be merged to that region.

The result of the previous processes frequently produces several regions with few pixels each and therefore it is necessary to merge them. Hence, the decision to group regions was based on their spectral separability, estimated by the Jeffreys-Matusita (JM) distance [13], a common measure used in feature selection procedures.

Let R_A and R_B be two neighboring regions with respective mean vectors $\boldsymbol{M}_A$ and $\boldsymbol{M}_B$ and covariance matrices $\boldsymbol{C}_A$ and $\boldsymbol{C}_B$; the JM distance for normally distributed classes is given by:

$$JM_{A,B} = \sqrt{2(1-e^{-B})} \tag{1}$$

in which

$$B = \frac{1}{8}(M_A - M_B)^T \left\{\frac{C_A + C_B}{2}\right\}^{-1} \times (M_A - M_B) + \frac{1}{2}\ln\left\{\frac{\left|(C_A + C_B)/2\right|}{|C_A|^{1/2}|C_B|^{1/2}}\right\} \tag{2}$$

which is known as Bhattacharyya distance [14], where T = transposition function; ln = natural logarithm; || = determinant. JM distance values range from 0 to 2, with higher values indicating total separability between adjacent regions. Fig. 2 illustrates the process:

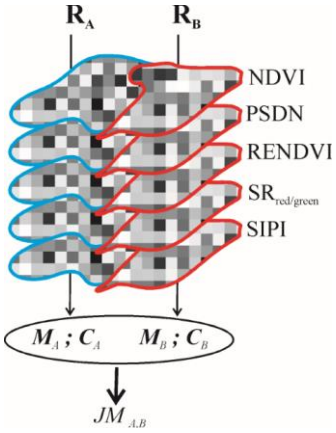

Fig. 2. Jeffreys-Matusita (JM) distance (Eq. 1) between regions R_A and R_B, calculated with mean vectors ($\boldsymbol{M}_A$; $\boldsymbol{M}_B$) and covariance matrices ($\boldsymbol{C}_A$; $\boldsymbol{C}_B$). Finally, a region R_A will be grouped to a neighbor R_B if the following conditions are satisfied:

i) $||M_A - M_B|| < p\_T$, with p_T updated iteratively until T is reached;

ii) $JM_{A,B} \leq JM_{threshold}$.

After a set of empirical tests, the combination of parameters for the segmentation algorithm that produced the best results was: T=30; minimum size of a region = 30 pixels; $JM_{threshold}$=0.5 and ex= 15.

2.2 Segmentation evaluation

To evaluate the segmentation results, ITCs of semi-deciduous tree species were manually delineated in the 3 test areas using a true color composite (R= 638 nm; G=548 nm; B=460 nm) and a fixed scale of 1:2000. First, we computed the percentage of the area of the segments inside each reference ITC, say $\boldsymbol{\theta}$. Therewith, it was verified the degree of fragmentation inside the ITCs of the reference. However, it was noted that some segments reached a $\boldsymbol{\theta}$ of 100 %, which means that 100 % of their area was located inside a reference ITC. A visual inspection of those segments reveled that they were related to spurious isolated pixels, located mainly in the borders of the images. In order to overcome this problem, a second score, $\boldsymbol{\mu}$, was computed, which is referred as the percentage of reference ITC´s area occupied by a given region. The larger $\boldsymbol{\theta}$ and $\boldsymbol{\mu}$, the better the segmentation is. Finally, we define:

$$\boldsymbol{\varphi} = \frac{\textit{number of segments with } \theta \geq 50\% \textit{ and } \mu \geq 75\%}{\textit{number of ITCs of the reference}} \qquad (4)$$

The score $\boldsymbol{\varphi}$ ranges from 0 to 1, being 1 a perfect segmentation (i.e. all of the reference ITCs were perfect outlined by the algorithm). Thus, we count the number of segments with more than 50% of their area inside a reference ITC and the segment´s area should overlap 75% or more of the reference ITC´s area.

3. RESULTS AND CONCLUSION

Results of the accuracy score $\boldsymbol{\varphi}$ for the test regions 1, 2 and 3 reached 55%, 56% and 70%, respectively, indicating the percentage of ITCs well delineated by the algorithm. It is worth noting that the score $\boldsymbol{\varphi}$ is quite restrictive due to the numerator of Eq. 4. Fig. 3 shows the results for the test region 3. Segments that meet the criterion presented in Eq. 4 are depicted in red color and coincide in size and shape with the manually delineated ITCs.

For semi-deciduous tree species, particularly in the dry season (when the hyperspectral images were acquired), leaf anthocyanin content tends to be higher due to the senescence process. This causes an increase in reflectance values at the red region, ascribing a reddish aspect to tree crowns (Figure 3a). For instance, as $SR_{red/green}$ is directly proportional to red reflectance, deciduous tree species stand out from other species (Figure 3b). The segmentation algorithm was functional to detect this pattern and successfully identified ITCs. This suggests that the method could be applied to data acquired from high spatial resolution spaceborne sensors, with broad bands centered at green and red regions.

Although further tests must be performed to prove the effectiveness of the segmentation algorithm, promising results were achieved. The spectral separability measure (i.e. JM distance) employed to merge segments proved to be a useful criterion on the ITC delineation process. This, together with the computation of VIs, is a simple way to explore the high dimensionality of hyperspectral data. Future work will focus on ITC delineation of evergreen tree species and at the applicability of the segmentation algorithm on object-oriented classification approaches to map canopy tree species in tropical forests.

4. ACKNOWLEDGMENTS

We thank the São Paulo Research Foundation (FAPESP) grant number 2013/11.589-5 and the Coordination for the Improvement of Higher Education Personnel (CAPES) for supporting this work.

5. REFERENCES

[1] M.L. Clark, D.A. Roberts, and D.B. Clark, "Hyperspectral discrimination of tropical rain forest tree species at leaf to crown scales," *Remote Sens. Environ.*, vol. 96, no. 3-4, pp. 375-398, Jun. 2006.

[2] J.B. Féret, G.P. Asner, "Tree Species Discrimination in Tropical Forests Using Airborne Imaging Spectroscopy," *IEEE Trans. Geosci. Remote Sens.*, vol. 51, no. 1, pp. 73–83, Jan. 2013.

[3] M.P. Ferreira, A.E.B. Grondona, S.B. Rolim and Y. E. Shimabukuro, "Analyzing the spectral variability of tropical tree species using hyperspectral feature selection and leaf optical modeling," *Journal of Applied Remote Sensing*, vol. 1, pp. 073502-1-073502-13, 2013.

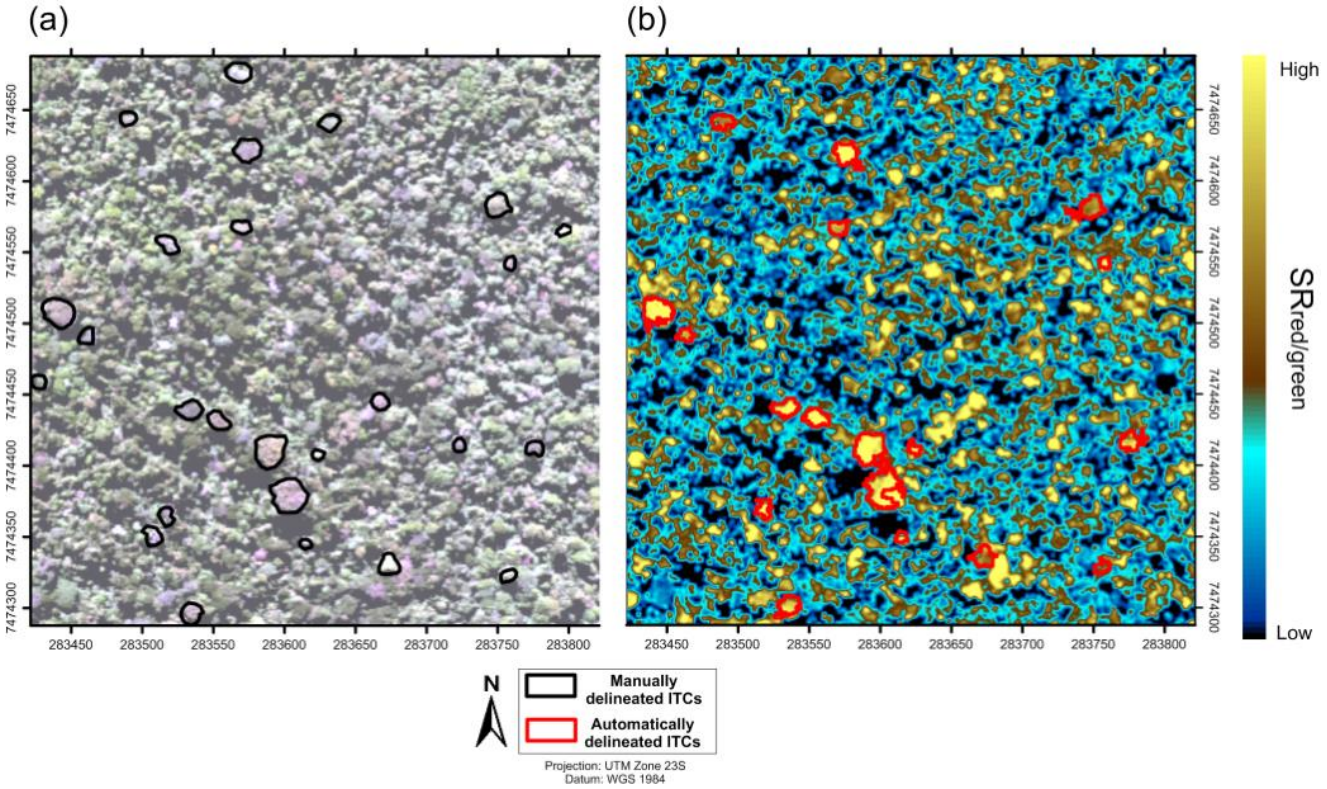

Fig. 3. (a) True color composite of area test 3 (R= 638 nm; G=548 nm; B=460 nm) with manually delineated individual tree crowns (ITCs) depicted in black; (b) Image of the ratio between red (600-699 nm) and green (500-599 nm) broad bands ($SR_{red/green}$) showing automatically delineated ITCs. Outlines depicted in red match the criterion of Eq. 4 (see text for explanations).

[4] M. Dalponte, H.O. Ørka, L.T. Ene, T. Gobakken and E. Næsset, "Tree crown delineation and tree species classification in boreal forests using hyperspectral and ALS data," *Remote Sens. Environ.*, vol. 140, pp. 306-317, Jan. 2014.

[5] G. W. Felde, G. P. Anderson, S. M. Adler-Golden, N. W. Matthew and A. Berk,"Analysis of Hyperion data with the FLAASH atmospheric correction algorithm," in *Proc. Of IGARSS, 2006*.

[6] Y. E. Shimabukuro, and J. A. Smith. "The least-squares mixing models to generate fraction images derived from remote sensing multispectral data," *IEEE Transactions on Geoscience and Remote Sensing*, vol. 29, no. 1, pp. 16-20, 1991.

[7] J.W. Rouse, R.H. Haas, J.A. Schell, and D.W. Deering, "Monitoring vegetation systems in the Great Plains with ERTS," in Proc. of Third ERTS-1 Symposium, 1973.

[8] G.A. Blackburn, "Quantifying chlorophylls and carotenoids from leaf to canopy scale: anevaluation of some hyperspectral approaches," *Remote Sens. Environ.*, vol. 66, no. 3, pp. 273–285, Dec. 1998.

[9] A. A. Gitelson, M.N. Merzlyak and H.K. Lichtenthaler, "Detection of red edge position and chlorophyll content by reflectance measurements near 700 nm," *Journal of Plant Physiology*, vol. 148, no. 3–4, pp. 501−508, 1996.

[10] J.A. Gamon and J.S. Surfus, "Assessing Leaf Pigment Content and Activity With a Reflectometer," *New Phytologist*, no. 143, pp. 105-117, 1999.

[11] J. Penuelas, F. Baret and I. Filella, "Semiempirical indexes to assess carotenoids chlorophyll-a ratio from leaf spectral reflectance,".*Photosynthetica*, vol. 31, no. 2, pp.221−230, 1995.

[12] G. Câmara, R.C.M. Souza, U.M. Freitas, J. Garrido, "SPRING: Integrating remote sensing and GIS by object-oriented data modelling," *Computers & Graphics*, vol. 20, no.3, pp. 395−403, 1996.

[13] A.G.Wacker, 1971: The Minimum Distance Approach to Classification, Ph.D. Thesis, Purdue University,West Lafayette.

[14] T. Kailath, "The divergence and Bhattacharyya distance measures in signalselection," *IEEE Trans. Commun. Technol.*, vol. 15, no. 1, pp. 52–60,Feb. 1967.